

Report from the Multi-Messenger Working Group at UHECR-2014 Conference

Timo KARG¹ for the IceCube Collaboration⁶

Jaime ALVAREZ-MUÑOZ², Daniel KUEMPEL³ and Mariangela SETTIMO⁴ for the Pierre Auger Collaboration⁷

Grigory RUBTSOV⁵ and Sergey TROITSKY⁵ for the Telescope Array Collaboration⁸

¹*DESY, Platanenallee 6, Zeuthen, Germany*

²*Universidad de Santiago de Compostela, Santiago de Compostela, Spain*

³*III. Physikalisches Institut A, RWTH Aachen University, Sommerfeldstraße, Aachen, Germany*

⁴*Laboratoire de Physique Nucléaire et de Hautes Energies (LPNHE), Universités Paris 6 et Paris 7, CNRS-IN2P3, Paris, France*

⁵*Institute for Nuclear Research of the Russian Academy of Sciences, Moscow, Russia*

⁶<https://icecube.wisc.edu/collaboration/authors/2015/04>

⁷http://www.auger.org/archive/authors_2015_04.html

⁸<http://www.telescopearray.org/index.php/research/collaborators>

E-mail: timo.karg@desy.de, jaime.alvarezmuniz@gmail.com, kuempel@physik.rwth-aachen.de, mariangela.settimo@lpnhe.in2p3.fr, grisha@ms2.inr.ac.ru, sergey.troitsky@gmail.com

The IceCube, Pierre Auger and Telescope Array Collaborations have recently reported results on neutral particles (neutrons, photons and neutrinos) which complement the measurements on charged primary cosmic rays at ultra-high energy. The complementarity between these messengers and between their detections are outlined. The current status of their search is reviewed and a cross-correlation analysis between the available results is performed. The expectations for photon and neutrino detections in the near future are also presented.

KEYWORDS: UHECR 2014, multi-messenger, neutron, neutrino, photon

1. Introduction

The most energetic and violent, but also less understood, astrophysical objects in the Universe are expected to produce non-thermal radiation of hadronic origin, with an accompanied flux of gamma-rays and neutrinos. The simultaneous observation of these particles - the so-called multi-messenger approach - is a key ingredient for discovering the sources themselves, and for better understanding the underlying mechanisms responsible for their violent activity.

High-energy multi-messenger astronomy has entered an exciting era, with the development and operation of new detectors offering unprecedented opportunities to observe cosmic radiation in the Universe, and with the successful detection of gamma-rays and neutrinos with energies $10^{14} - 10^{15}$ eV, at the lower edge of the high-energy Universe we hope to observe in the future.

The aim of this contribution is to review the status of high-energy gamma-ray, neutron, and neutrino observations, as well as to provide prospects for future observations, with a focus on the energy range from 10^{15} eV up to the highest energy ever observed in a single particle $\sim 10^{20}$ eV.

2. Multi-messenger particles

Identifying the sources of very high-energy (VHE $10^{15} - 10^{18}$ eV) and ultra-high energy (UHE $> 10^{18}$ eV = 1 EeV) cosmic rays (CRs) is one of the key problems in Astroparticle Physics. Being charged particles, cosmic rays are deflected in the galactic and extragalactic magnetic fields and lose information about the position of the site where they were produced, unless they are light nuclei and have energies above a few tens of EeV. However, even at these energies (more precisely above $\sim 5 \times 10^{19}$ eV), cosmic rays are expected to interact with the Cosmic Microwave Background (CMB) radiation [1, 2], that limits their observability to distances smaller than 50-100 Mpc, representing a small fraction of the observable volume of the Universe. Fortunately, high-energy photons and neutrinos are expected to be produced by cosmic rays at/around their sources as well as in their propagation in the Universe through neutral and charged pion production and their successive decay.

As neutral particles, photons and neutrinos propagate undeflected by magnetic fields, pointing back to their production sites, including the sources of the CRs. This makes them suitable candidates to extend astronomical observations to unprecedented energy ranges. Moreover, if the sources of CRs are transient, typically involving compact objects (such as gamma-ray bursts), an observation of photons and neutrinos (and possibly gravitational waves) could in fact be the only path that might lead to a full understanding of the underlying processes.

Photons (up to ~ 100 TeV) have been observed from a variety of sources [3]. Their detection is already providing important clues on the origin of the very-high energy cosmic rays, with the hadronic origin of the observed gamma-rays favored with respect to the leptonic model in a few cases [4]. Unfortunately, the absorption of gamma-rays by electron-positron pair production with the low energy photons of the extragalactic background radiation (infrared, CMB and radio) limits their observability to the local Universe. The effect is energy-dependent, with photons at energies around 10^{15} eV having a horizon distance of order of the Milky Way size, while UHE photons at 10 EeV are detectable from distances of ~ 10 Mpc.

High-energy neutrinos can escape from denser and deeper environments than photons, and propagate unaltered through the Universe with virtually no limit to their observation distance regardless of their energy. Neutrinos can provide important information about the processes taking place in astrophysical engines and could even reveal the existence of sources opaque to hadrons and photons, sources that would thus far have remained undetected. VHE neutrinos of cosmic origin, with energies up to 2 PeV, have recently been observed, for the first time, with the IceCube experiment [5]. Their detection represents an important milestone and a major step towards multi-messenger astronomy. Unfortunately, due to the nature of the detected events, identification of their sources has not been yet possible (cf. Sec. 3.2), even if natural candidates are the identified sources of TeV photons.

In the UHE range, around 1 EeV and above, neutrinos and gamma-rays have so far escaped detection by existing experiments and only upper limits to their fluxes exist. An expected “guaranteed” source of UHE photons and neutrinos is the interaction of UHECRs with the CMB. The fluxes are uncertain mainly due to the unknown energy spectrum and composition of the primary cosmic ray beam, and due to the evolution with redshift and spatial distribution of the sources. On the other hand, and thanks to these dependencies, the observation of UHE photons and neutrinos would provide further hints on the features of UHECR sources [6]. Furthermore in the UHE range, top-down models, in which the pions producing photons and neutrinos arise from the decay or annihilation of exotic particles, are strongly constrained by searches for UHE photons and neutrinos [7–9].

In the following, we give a brief introduction to the observatories involved in this report.

The IceCube Neutrino Observatory (IceCube) has been installed at depths between 1450 m and 2450 m in the Antarctic ice sheet at the geographic South Pole. It comprises 86 vertical strings with a

typical inter-string spacing of 125 m, each one instrumented with 60 digital optical modules (DOMs) [10]. IceCube is optimized to measure Cherenkov radiation from charged particles produced in TeV to PeV neutrino interactions inside or close to the 1 km^3 of instrumented ice.

On the surface above the deep ice detector, an array of 81 stations, IceTop [11], measures charged particles from extensive air showers induced by cosmic rays in the energy range from 300 TeV to $> 1 \text{ EeV}$. In a limited zenith angle range, IceTop can also be utilized as a veto against atmospheric muons in the deep ice detector, which constitute the largest source of background for neutrino searches, and vice versa for searches for muon-poor showers that constitute high-energy photon candidates.

The Pierre Auger Observatory (Auger) is located in the Province of Mendoza, Argentina, at a mean altitude of 1400 m (atmospheric overburden of $\sim 875 \text{ g cm}^{-2}$) [12] and sensitive to primary particles of UHE. The Observatory is a hybrid system, a combination of a large surface detector array (SD) and a fluorescence detector (FD). The SD is composed of over 1660 water-Cherenkov stations placed in a triangular grid with nearest neighbors separated by 1500 m, and spread over an area of $\sim 3000 \text{ km}^2$. The 27 telescopes of the FD overlook the SD from five sites. The SD was used to search for UHE neutrinos (cf. Sec. 3.2), while both the SD and FD were used to search for UHE photons (cf. Sec. 3.3).

The Telescope Array (TA) experiment is located in Millard County, Utah, USA and optimized for detecting UHE particles. It consists of the surface detector with 507 scintillators covering an area of approximately 700 km^2 overlooked by 38 fluorescence telescopes located at three sites [13, 14]. The TA fluorescence telescopes operate in hybrid mode with the surface detector and at the same time allow monocular and stereo reconstruction of the events.

3. Results

3.1 Neutron searches

Given the limited lifetime of free neutrons at rest of about 886 s, the mean travel distance is limited for relativistic neutrons to $9.2 \times E \text{ kpc}$, where E is the energy of the neutron in EeV. For energies above 2 EeV most of the galactic disk is in reach for neutron astronomy while the galactic center is already in range of 1 EeV neutrons. In the energy range of a few EeV Auger, HiRes, and Telescope Array have found their data consistent with a significant component of protons [15–18]. If sources in the galaxy are emitting protons up to the ankle in the energy spectrum, they could show themselves through a flux of primary neutrons produced by pion photo-production and nuclear interactions of the protons near the source.

Neutron induced air showers are indistinguishable from air showers produced by primary protons. However, since they are not deflected by magnetic fields, the signature of a primary neutron flux is an excess of hadronic air showers from a specific celestial direction. This complements the search for a directional excess of photons discussed in Sec. 3.3 where dedicated discrimination techniques are applied. Both the Pierre Auger Observatory and Telescope Array searched for an excess of events in the southern and northern hemisphere, respectively. No statistically significant excess has been found in any small solid angle that would be indicative of a flux of neutral particles from a discrete source [19, 20]. In the case of the Pierre Auger Observatory the search covers a declination band from -90° to $+15^\circ$ in four different energy ranges above 1 EeV. With a total exposure of $24,880 \text{ km}^2 \text{ sr yr}$ flux upper limits of neutral particles have been placed in the exposed sky and are displayed in Fig. 1 (left). The typical (median) flux upper limit above 1 EeV is $0.0114 \text{ neutron km}^{-2} \text{ yr}^{-1}$ corresponding to an energy flux limit of $0.083 \text{ eV cm}^{-2} \text{ s}^{-1}$. In case of the Telescope Array experiment, a search is performed in a declination band from 0° to 70° in four different energy ranges starting from 0.5 EeV. A significance map derived from TA events is shown in Fig. 1 (right). The averaged point source flux

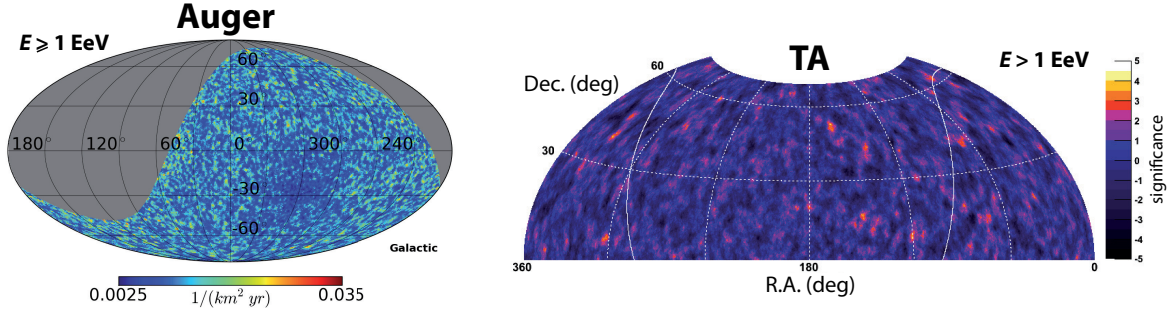


Fig. 1. **Left:** Celestial map of the flux upper limit (particles $\text{km}^{-2} \text{yr}^{-1}$) for neutral particles of Auger in galactic coordinates [19]. **Right:** Significance map of neutral particles of TA in equatorial coordinates [20].

upper limit in the northern sky is $0.07 \text{ neutrons km}^{-2} \text{yr}^{-1}$ [20] for the energy greater than 1 EeV.

To limit the statistical penalty for making many trials (as in the blind search analyses described above) classes of objects of potential sources of neutrons are tested in a separate targeted search [21]. In total, nine target sets of candidate sources of a given class are combined in a “stacking analysis”. The signal should be more significant than that of a single target by itself under the hypothesis that many (or all) of the candidate sources are indeed emitting neutrons. In addition the galactic center and the galactic plane region are considered as additional stand-alone targets. None of the candidate source classes tested revealed compelling evidence for EeV neutrons. Upper limits from the galactic plane constrain models for continuous production of EeV protons in the Galaxy.

3.2 Neutrino searches

In 2013 IceCube reported the detection of two neutrino candidates with estimated deposited energies of 1 PeV [22]. These events were discovered in a search for extremely high energy (EHE) neutrinos, that used simple selection cuts on the total amount of light and the reconstructed zenith angle to suppress the atmospheric muon and neutrino backgrounds. At that time the significance for the two PeV-events not being of atmospheric origin was 2.8σ [22], and the up-to-today most stringent upper limits on the neutrino flux between 1 PeV and 200 PeV could be derived [23] as shown in Fig. 2 (left). Both observed PeV neutrino events appear cascade-like, i.e. neutrinos interacting inside the instrumented volume without an outgoing muon track, and the photon timing distribution in the detector suggests that both events are down-going, i.e. originating in the southern hemisphere. These observations prompted the development of a novel search method: Selecting bright events that start inside the instrumented volume with the outer layers of DOMs acting as a veto that allows the suppression of atmospheric muons by 10^{-5} [24]. While atmospheric neutrinos from the northern hemisphere constitute an irreducible background, atmospheric neutrinos from the southern hemisphere can be efficiently suppressed by using self-veto techniques, that involves tagging them via high energy muons originating from the same air shower [25, 26]. Applying this search method to three years of IceCube data revealed 37 high-energy neutrino candidates with deposited energies between 30 TeV and 2 PeV. The null-hypothesis of a purely atmospheric origin is rejected at 5.7σ and, assuming an unbroken E^{-2} spectrum, the best-fit per-flavour astrophysical flux is $E^2\phi(E) = (0.95 \pm 0.3) \cdot 10^{-8} \text{ GeV cm}^{-2} \text{ s}^{-1} \text{ sr}^{-1}$ [5]. Up to today, no source of these astrophysical neutrino flux could be identified; the data are consistent with expectations for equal fluxes of all three neutrino flavours [27] and with isotropic arrival directions [5]. A multi-messenger analysis to correlate the observed neutrinos with UHE charged cosmic rays measured by the Pierre Auger Observatory and Telescope Array is in preparation [28].

A search for neutrinos in the energy range around 1 EeV and above has been performed with events detected by the surface detector of the Pierre Auger Observatory. While protons, heavier nuclei, and photons interact shortly after entering the atmosphere, neutrinos can initiate showers close to the ground level. At large zenith angles the atmosphere is thick enough so that the electromagnetic component of nucleonic cosmic ray-induced showers gets absorbed and the shower front at ground level is dominated by muons. On the other hand, showers induced by neutrinos deep in the atmosphere have a substantial electromagnetic component at the ground. The current SD is not directly sensitive to the muonic and electromagnetic components of the shower separately, nor to the depth at which the shower is initiated. However the digitization of the signals induced by the passage of shower particles with Flash Analog to Digital Converters (FADC) with 25 ns time resolution allows one to distinguish narrow signals in time (such as those present in inclined showers initiated high in the atmosphere), from the broad signals expected in inclined showers initiated close to the ground. Applying this simple idea we can efficiently detect inclined showers and search for (a) Earth-skimming (ES) showers induced by tau neutrinos (ν_τ) that travel in the upward direction with respect to the vertical to ground, and (b) downward-going (DG) showers initiated by any neutrino flavour at large zenith angles and that interact in the atmosphere close to the SD. Typically, only Earth-skimming ν_τ -induced showers with zenith angles $90^\circ < \theta < 95^\circ$ and downward-going showers with $\theta > 60^\circ$ may be identified with large efficiency. The identification of potential neutrino-induced showers is based on first selecting those events that arrive in rather inclined directions, and then selecting among them those with FADC traces that are spread in time, indicative of the early stage of development of the shower and a clear signature of a deeply interacting neutrino triggering the SD. Full details of the procedure are given in [8, 9, 29].

A novel approach with respect to previous publications [8, 9] has been implemented in the analysis for the first time by combining searches in the ES and DG channels together using a simple procedure (see [29, 30] for details). In this way the exposure to UHE neutrinos is enhanced with respect to that obtained when each channel is considered separately. A strong background reduction against showers initiated by UHE cosmic rays is possible. The search for UHE neutrinos at the Auger Observatory is limited by exposure but not by background. The ES and DG criteria were applied to data between 1 January 2004 up to 31 December 2012 (excluding data periods used to train the selections) with no neutrino candidates found.

For the calculation of the exposure of the SD to UHE neutrinos, the same set of trigger and neutrino identification conditions that were applied to data are also applied to the simulated neutrino showers. Using the combined exposure and assuming a differential neutrino flux $dN(E_\nu)/dE_\nu = k \cdot E_\nu^{-2}$ as well as a $\nu_e : \nu_\mu : \nu_\tau = 1 : 1 : 1$ flavour ratio, an upper limit on the value of k at 90% C.L. was obtained through a standard procedure [31]: $E^2 dN/dE < 1.3 \times 10^{-8} \text{ GeV cm}^{-2} \text{ s}^{-1} \text{ sr}^{-1}$. This is below the normalization of the Waxman-Bahcall landmark [32]. Auger is the first shower array to reach that level of sensitivity (cf. page 79, Fig. 5 in [29]). The limit is displayed in differential format in Fig. 2 (left), where the Auger limit integrated in bins of width 0.5 in $\log_{10} E_\nu$ is presented, along with those from other experiments [23, 33]. As can be seen in Fig. 2 (left), the maximum sensitivity of Auger is achieved at $\sim \text{EeV}$ neutrino energy where most cosmogenic models of ν production also peak (in an E_ν^2 times flux plot). The result is finalized with more data until 20 June 2013 in [30]. The Auger limit places strong constraints on cosmogenic ν models that assume a pure primary proton composition injected at the sources and strong (FRII-type) evolution of the sources [36]. Auger is less sensitive to the cosmogenic neutrino models represented by the gray shaded area in Fig. 2 which brackets the lower fluxes predicted under a range of assumptions [6]. The same remark applies to models that assume pure-iron composition at the sources.

No neutrino sources have been identified, yet. While Auger is sensitive to neutrinos with ener-

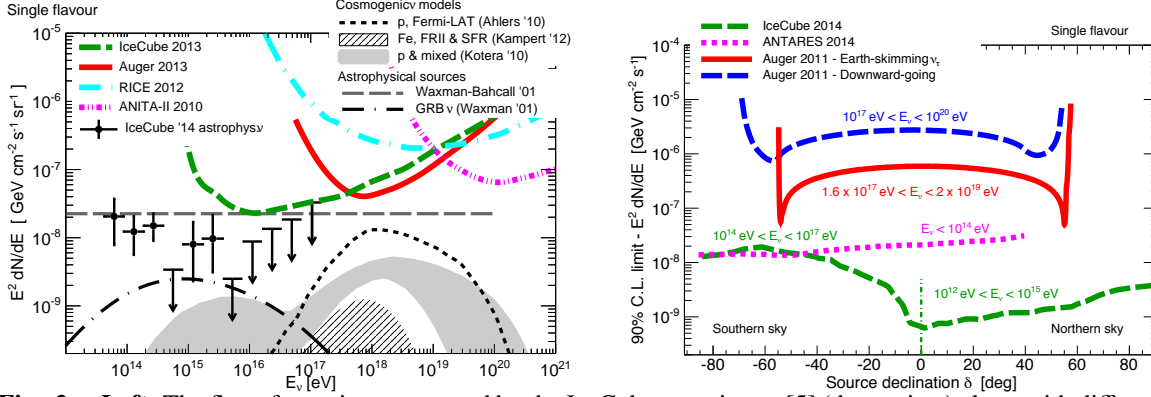


Fig. 2. **Left:** The flux of neutrinos measured by the IceCube experiment [5] (data points) along with different upper limits from the Pierre Auger Observatory [29], ANITA-II [33], IceCube [23] and RICE [34] experiments (all limits converted to single flavour and 90% C.L. and shown in bins of width 0.5 in $\log_{10} E_\nu$ – except for the RICE limit that is calculated as explained in [35]). Also shown are the expected neutrino fluxes for several cosmogenic neutrino models [6, 36, 37] as well as the Waxman-Bahcall bound [32]. **Right:** Upper limits (at 90% C.L.) on the single-flavour neutrino flux from point-like sources for different declinations derived from non-observations in the Auger [38], IceCube [39], and ANTARES [40] experiments. In all cases an unbroken E^{-2} energy spectrum is assumed. For southern hemisphere sources with a high-energy cut-off, IceCube is less sensitive.

gies larger than 100 PeV, IceCube can extract a very pure TeV-neutrino sample from the northern hemisphere which is dominated by atmospheric neutrinos and a sample of high-energy (100 TeV to 100 PeV) neutrino-candidate events in the southern hemisphere. In the Auger Observatory no neutrino candidates were found [38]. IceCube has performed dedicated searches for spatial clustering of neutrino candidate events but no significant clustering of the arrival directions has been observed [39]. Upper limits on the flux from point-like neutrino sources are calculated by both experiments and illustrated in Fig. 2 (right). The resulting 90% C.L. upper limits are shown as a function of declination. For the southern hemisphere the most stringent limits are set by the ANTARES neutrino telescope in the Mediterranean Sea, especially for sources with a high-energy cut-off which is expected for Galactic neutrino sources [40].

3.3 Photon searches

Given their mostly electromagnetic nature, on average, photon-induced air showers develop deeper in the atmosphere, compared to hadron-induced ones of similar energies. In addition, a significantly smaller muon content, compared to hadron induced showers, is expected. As a consequence, photon induced showers at EeV energies have a smaller signal in the surface detectors, a steeper lateral distribution of secondary particles, a narrower distribution of arrival times of particles in the shower front and a larger delay with respect to a planar shower front approximation. These differences are further enhanced at energies above 10^{19} eV because of the Landau-Pomeranchuk-Migdal (LPM) effect [41, 42]. The development of the air shower is then slowed and the event by event fluctuations are enhanced [43, 44]. At energies above ~ 50 EeV, photons entering the geomagnetic field can convert to electron-positron pairs with a probability that depends on the energy of photons and on the component of the local magnetic field orthogonal to the particle motion [45, 46]. A bunch of low-energy electromagnetic particles, called a “preshower”, thus enters the atmosphere and is detected as a single shower developing higher in atmosphere and with a flatter lateral distribution.

Diffuse photon searches at ultra-high energy

Searches for photons have been performed by the Auger and the TA collaborations. No primary photons have been unambiguously identified so far above the EeV energies and upper limits have been placed on the diffuse photon fraction and integral photon flux by several experiments [7, 47–53]. Above 10^{19} eV, both Auger and TA have performed a search for photon-induced showers using the respective surface detectors. The mass sensitive observables in the two analyses are related to the curvature of the shower front and, in the case of Auger, also to the time spread of particles (see [7, 49] for details). At energies lower than 10^{19} eV, upper limits on the integral flux of photons are derived by Auger using events detected with the fluorescence telescopes operating in hybrid mode. These events benefit from the low energy threshold of the direct observation of the depth at which the energy deposit reaches its maximum (X_{\max}) with the FD and of complementary informations from SD [50]. An analysis based on the observation of X_{\max} with hybrid events is in progress within the TA collaboration.

The current upper limits on the integral photon flux are shown in Fig. 3 as a function of the energy reconstructed assuming that the primary particle is a photon. In fact, while for hybrid events the energy is directly measured by FD in a calorimetric way, for SD events the energy estimator is the signal at a reference distance r_{opt} specific to each experimental layout and the SD detector. The difference in the development between the bulk of air showers and potential rare photon-induced events results in incorrect determination of the energy for primary photons [54, 55]. This effect is taken into account and all modern constraints on the flux of primary UHE photons use the appropriate energy scale for photon primaries. The tighter limits found by Auger, compared to TA, reflect the differences in the detectors and in the exposure of the two experiments: (i) the exposure of TA is about a factor 7 smaller than that of Auger; (ii) compared to scintillators, the water-Cherenkov stations are more sensitive to muons, so that they detect weaker signals from the muon-poor photon induced showers, enhancing the photon/hadron separation capabilities. Moreover the two experiments, located in different hemispheres, have quite different and complementary fields of view, so a direct comparison should be taken with care.

The current results disfavor the exotic models for the origin of UHECR described in [56, 57] over a wide energy range while the region of expected GZK photon fluxes in the most optimistic scenario can be explored by Auger in the very near future, cf. Fig. 3 (left).

Diffuse photon searches at TeV – PeV energy

Following the multi-messenger paradigm that cosmic rays, photons and neutrinos are produced in the same hadronic processes in the sources, the recent discovery of an excess of high-energy neutrinos over the atmospheric background (cf. Sec. 3.2) has attracted considerable interest [65–70] to searches for a diffuse photon flux at PeV energies. Experimental constraints on the diffuse flux of sub-PeV to sub-EeV photons are presented in Fig. 3 (right) together with predictions from models. Note that EAS-MSU reported a claim of detection of cosmic gamma rays above PeV energies [64]. However, the KASCADE-Grande experiment did not find any signal in the same energy range with similar sensitivity [71], cf. Fig. 3 (right).

The IceCube Observatory also is sensitive to PeV photons by looking for muon-poor showers in the deep ice-detector. A search has been performed with the 40 string configuration in the declination region $-90^\circ < \delta < -60^\circ$ [72]. No correlation of photon candidates with the Galactic plane was found and an upper limit on the photon fraction of $1.2 \cdot 10^{-3}$ was set in the energy range from 1.2 to 6 PeV. Further, no clustering of photon candidate events was observed in a search for point-like sources in the complete field of view. A similar analysis with the full IceCube detector is in preparation.

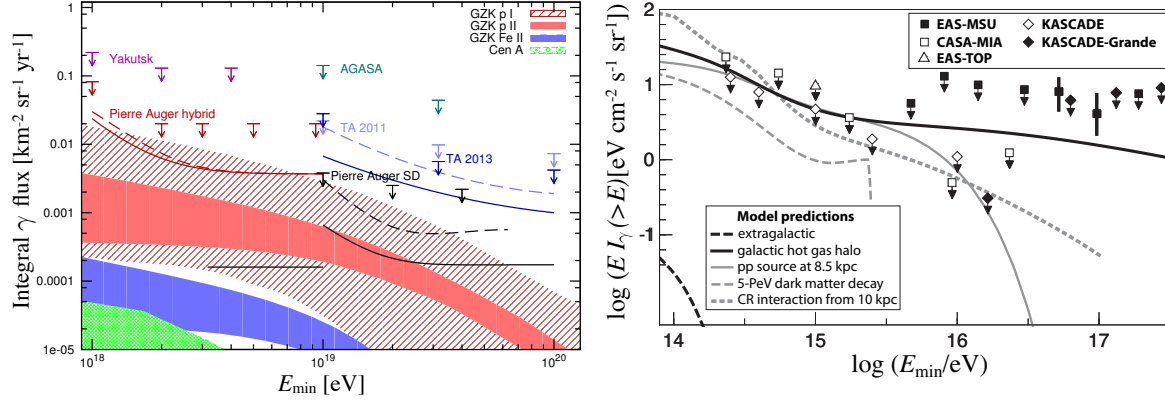


Fig. 3. **Left:** 95% C.L. upper limits on the integral UHE photon flux derived by Auger with the hybrid [50] and SD [7] detectors and TA SD detector [49], compared to the results of AGASA [51] and Yakutsk [52]. The shaded regions give the predictions for the GZK photon flux models from [56] assuming protons at the source (red shaded), from [58] (red and blue, under the assumption of proton and iron acceleration), and for the case of a single source as Centaurus A [59] (green). Sensitivity expectations of the year 2020 for Auger and TA are indicated by dashed and solid lines, cf. Sec. 5 for more details. **Right:** PeV to EeV constraints on the diffuse photon flux. Fluxes are obtained assuming isotropic emission; data from EAS-TOP (90% C.L.) [60], KASCADE (C.L. not quoted) [61, 62], KASCADE-Grande (90% C.L.) [71], CASA-MIA (90% C.L.) [63] and EAS-MSU (95% C.L.) [64]. Systematic errors for all these results, mostly related to simulations of the background contamination, are of order $\pm 50\%$. Lines represent some model predictions constrained by the IceCube measured neutrino flux: extragalactic [65], Galactic hot gas halo [65], pp source at a fixed distance of 8.5 kpc [66], 5-PeV dark matter decay [66], cosmic-ray interactions with interstellar matter at a fixed distance of 10 kpc [67].

Directional photon searches

Similar to the search for a directional excess of neutrons discussed in Sec. 3.1, ultra-high energy photons, produced in vicinity of a potential source, can be detected by an accumulation of events from a specific target direction. Since photon induced air-showers exhibit specific characteristics, the sensitivity for detection can additionally be improved by selecting only “photon-like” events. Compared to EeV neutrons, the detectable volume is large enough to encompass in addition to the Milky Way, the Local Group of galaxies, and possibly Centaurus A, given an attenuation length of about 4.5 Mpc at EeV energies [73–75].

Data from the Pierre Auger Observatory was used to search for an excess of photon-like events from 526,200 target directions (target separation $\sim 0.3^\circ$) between a declination range of -85° and $+20^\circ$ in the energy range of $10^{17.3}$ eV up to $10^{18.5}$ eV [76]. To select photon-like events, five photon-sensitive observables from the surface detector array as well as from the fluorescence detector are combined in a multivariate analysis using boosted decision trees [77, 78]. Details on the photon-like events selection and on the statistical methods used to derive the p -value (local probability that the data is in agreement with a uniform distribution) and the upper limits on the photon flux are given in [76]. No statistical evidence for any target direction has been found. The mean value for the upper limit at 90% C.L. is $0.035 \text{ photons km}^{-2} \text{ yr}^{-1}$, with a maximum of $0.14 \text{ photons km}^{-2} \text{ yr}^{-1}$ as shown in Fig. 4. Those values correspond to an energy flux of $0.06 \text{ eV cm}^{-2} \text{ s}^{-1}$ and $0.25 \text{ eV cm}^{-2} \text{ s}^{-1}$, respectively, assuming an E^{-2} energy spectrum.

The limits are of considerable astrophysical interest. By extrapolating measured energy fluxes

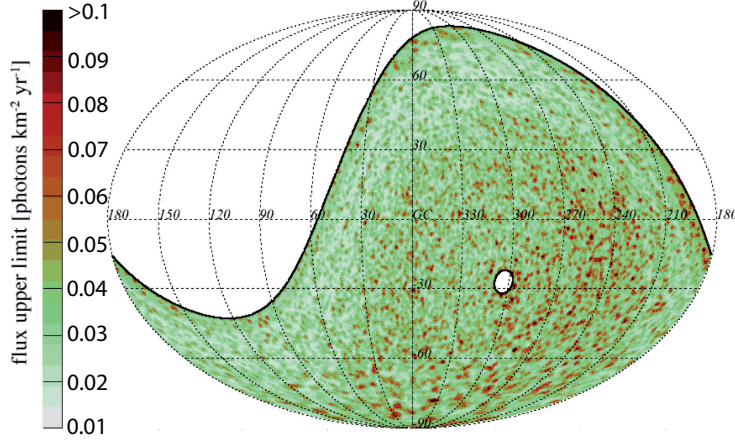


Fig. 4. Celestial map of photon flux upper limits in photons $\text{km}^{-2} \text{yr}^{-1}$ illustrated in Galactic coordinates. [76]

at TeV energies (e.g. [79, 80]) assuming a spectral index of E^{-2} this flux would have been detected with more than 5σ significance, even after penalizing for the large number of trials. Furthermore, making conservative assumptions for median exposure targets one can exclude a photon flux greater than $1.44 \text{ eV cm}^{-2} \text{ s}^{-1}$ with 5σ significance. The null result from this search does not mean that the sources of EeV cosmic rays are extragalactic as they might be produced for example by transient sources where the Earth was not exposed during the collection of data or continuous sources in the Galaxy which emit in jets that do not point towards the Earth.

The directional photon search is also underway in TA.

4. Cross-correlation analysis between Auger and TA

As we have already pointed out, Auger and TA are complementary in the photon search both by their fields of view and by techniques. However, in the declination band of $-20^\circ < \text{dec} < +20^\circ$ both experiments have considerable exposure. Neither Auger nor TA have seen an excess of photon-like events, from any direction, statistically significant in a full-sky search, penalized for the fact that no particular direction is a priori expected to host a source. There exist, however, local excesses of photon-like events in the Auger data and a number of photon candidates in the TA data. The directions to these excesses should be uncorrelated if they are just statistical fluctuations while a directional coincidence between local excesses of photon-like events seen by two independent experiments may indicate, if significant, the existence of a real UHE gamma-ray source. The purpose of the joint Auger+TA study, whose preliminary results are presented here for the first time, is to search for such possible correlations by looking for statistically significant excesses of Auger photon-like events from the directions of TA photon candidates. For this analysis, we use preliminary arrival directions of 9 TA surface detector photon-like events with energies $E_\gamma > 10 \text{ EeV}$ and angular resolution of 1.4° and 8 TA hybrid photon-like events with $E > 2 \text{ EeV}$ and angular resolution of 0.9° in the common field of view described above. The bulk of events in the Auger data set have considerably lower energies ($10^{17.3} < E [\log(E/\text{eV})] < 10^{18.5}$), so this kind of analysis may constrain sources emitting photons in

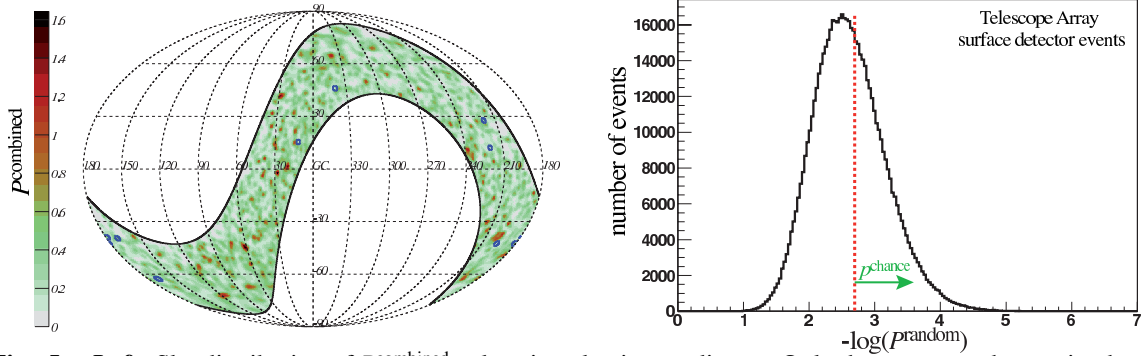


Fig. 5. **Left:** Sky distribution of P^{combined} values in galactic coordinates. Only the common observation band is shown. Blue circles indicate the position of 9 TA surface detector photon-like events with a radius according to their angular resolution. **Right:** Distribution of P^{random} values obtained from MC simulations. The red dashed line indicates the observed combined p -value of $-\log(P^{\text{combined}}) = 2.71$.

both energy ranges only.

To calculate the chance probability of the correlation of photon candidate events from the Pierre Auger Observatory and the Telescope Array the analysis is divided into several steps. First, a combined p -value is calculated from TA candidate directions. For n photon candidate events in the field of view of Auger with directions $(\alpha_1, \delta_1), (\alpha_2, \delta_2), \dots, (\alpha_n, \delta_n)$, P^{combined} is defined as

$$P^{\text{combined}} = \prod_n P^{\text{Auger}}(\alpha_n, \delta_n), \quad (1)$$

where P^{Auger} is the weighted average p -value from a specific direction. This value is obtained by weighting the actual p -value from [76] with a von Mises-Fisher distribution (vMF) [81] which incorporates in its concentration parameter the angular resolution of TA events.

To determine if the resulting P^{combined} is significantly small, mock P^{random} -values are obtained from MC simulations. These are calculated in the same way as in Eqn. 1 but using n randomly distributed arrival directions according to the acceptance of the TA detector. The last step is repeated $\sim 1,000,000$ times and the resulting distribution of P^{random} values is compared with P^{combined} by calculating the chance probability $p^{\text{chance}}(P^{\text{random}} \leq P^{\text{combined}})$.

The results of this analysis, using as an example the photon candidate events detected by the TA surface detector, are shown in Fig. 5. The corresponding chance probability is $p_{\text{SD}}^{\text{chance}} = 41\%$. Using photon-like events from the TA hybrid detector a chance probability of $p_{\text{Hy}}^{\text{chance}} = 68\%$ is obtained. Both analyses indicate that there is no statistically significant excess of photon candidate events when combining photon-like events from the Pierre Auger Observatory and Telescope Array in the commonly observed declination band. We must remark here that such result is not surprising since the photon-like events in the Auger data sample as well as the TA candidate events used as targets in the analysis, are mainly dominated by the nuclear background.

5. Summary and perspectives

In this contribution, we have reported about the status of the search for neutral primary cosmic rays with particular emphasis on the search for photons and neutrinos with Auger, Telescope Array and IceCube observatories. Whereas IceCube has observed a flux of astrophysical neutrinos, no UHE

photons and neutrinos have been identified by Auger and Telescope Array. A flux of such primary particles is expected as result of the UHECRs interaction with the CMB. A multi-messenger approach would provide strong constraints on the astrophysical scenarios as photon and neutrino fluxes are sensitive to different features of the source environment and of the cosmic-ray propagation. As already discussed, given the large exposure of the Auger Observatory, cosmogenic neutrino flux models are already being constrained, with detection of the first UHE cosmogenic neutrinos in reach in the next few years if the primary cosmic ray flux is dominated by protons. The Auger Observatory is most sensitive in an energy region complementary to the one where IceCube has its maximum detection capabilities. Also, planned experiments detecting radio waves in the MHz-GHz frequency range produced through the Askaryan effect in neutrino-induced showers (such as the Askaryan Radio Array – ARA [82] and ARIANNA [83]) have competing expected sensitivities to EeV neutrinos from cosmological origin. Last but not least, the analysis of data collected at the recent ANITA-III antenna-payload balloon flight is in progress.

To identify the sources of the astrophysical neutrinos an extension to IceCube, IceCube-Gen2, is currently being designed [84] in the southern hemisphere. With an instrument volume of about 10 km^3 it will be able to gather sufficient statistics with improved angular resolution to identify neutrino point sources or rule out many source classes. Further, it will allow us to precisely measure the energy spectrum and flavour composition of the diffuse neutrino flux. In the northern hemisphere, two km^3 -scale projects, KM3NeT [85] and Baikal-GVD [86], are under active development.

Interesting outcomes are expected in the near future also for photon primaries at ultra-high energy, as Auger will be able to explore the region of expected cosmogenic photon fluxes in the most optimistic astrophysical scenarios. The sensitivity to the photon flux expected in 2020 with Auger and TA is shown in Fig. 3 left (dashed and solid lines). The dashed lines are the extrapolations of the current analyses: compared to the estimates in [62], they take into account the detection of background events as derived from the current knowledge of the hadron-shower contamination. A significant boost of these sensitivities (solid lines) is possible with the upgrades of the Auger detectors [87] and the extensions of the TA array [88]. In the case of TA, the expected limits are derived assuming an improved analysis and three years of extension of the surface array by a factor 4. For Auger, an ideal scenario is shown, which includes new trigger algorithms, recently installed over the SD array, and the possible upgrade of the Observatory with muon detectors. Since a full analysis procedure is not yet established, the extrapolated limits are derived under the assumptions of 50% efficiency in photon selection and no detected photon and background events. Moreover, these results can have implications for fundamental physics since the predicted flux of GZK photons can be affected by Lorentz invariance violation (see for example [89,90]) or by possible photon-axion conversion [91,92] during photon propagation.

Combining the results of present and future instruments in a multi-messenger approach offers a chance to get insights on the cosmic ray puzzle within the next decade.

References

- [1] K. Greisen, *Phys. Rev. Lett.* **16** (1966) 748.
- [2] G. T. Zatsepin and V. A. Kuzmin, *JETP Lett.* **4** (1966) 78 [*Pisma Zh. Eksp. Teor. Fiz.* **4** (1966) 114].
- [3] J. Holder, *Astropart. Phys.* **39-40** (2012) 61.
- [4] M. Ackermann et al. (Fermi-LAT Collaboration), *Science* **339** (2013) 807.
- [5] M. G. Aartsen et al. (IceCube Collaboration), *Phys. Rev. Lett.* **113** (2014) 101101.
- [6] D. Allard, K. Kotera and A. Olinto, *JCAP* **10** (2010) 013.
- [7] J. Abraham et al. (Pierre Auger Collaboration), *Astropart. Phys.* **29** (2008) 243.
- [8] J. Abraham et al. *Phys. Rev. Lett.* **100** (2008) 211101; *Phys. Rev. D* **79** (2009) 102001; P. Abreu et al. *Astrophys. J. Lett.* **755** (2012) L4.

- [9] P. Abreu et al. (Pierre Auger Collaboration), Phys. Rev. D **84** (2011) 122005; J. L. Navarro, PhD Thesis, Univ. Granada, Spain (2012).
- [10] R. Abbasi et al. (IceCube Collaboration), Nucl. Instrum. Meth. A **601** (2009) 294.
- [11] R. Abbasi et al. (IceCube Collaboration), Nucl. Instrum. Meth. A **700** (2013) 188.
- [12] A. Aab et al. (Pierre Auger Collaboration), Nucl. Instrum. Meth. A **798** (2015) 172.
- [13] T. Abu-Zayyad et al. (Telescope Array Collaboration), Nucl. Instrum. Meth. A **689** (2012) 87.
- [14] H. Tokuno et al. (Telescope Array Collaboration), Nucl. Instrum. Meth. A **676** (2012) 54.
- [15] P. Abreu et al. (Pierre Auger Collaboration), Phys. Rev. Lett. **109** (2012) 062002.
- [16] J. Abraham et al. (Pierre Auger Collaboration), Phys. Rev. Lett. **104** (2010) 091101.
- [17] R. U. Abbasi et al. (HiRes Collaboration), Phys. Rev. Lett. **104** (2010) 0161101.
- [18] C. C. H. Jui for the Telescope Array Collaboration, J. Phys.: Conf. Ser. **404** (2012) 012037.
- [19] P. Abreu et al. (Pierre Auger Collaboration), Astrophys. J. **760** (2012) 148.
- [20] R. U. Abbasi et al. (Telescope Array Collaboration), arXiv:1407.6145 [astro-ph.HE].
- [21] A. Aab et al. (Pierre Auger Collaboration), Astrophys. J. Lett. **789** (2014) L34.
- [22] M. G. Aartsen et al. (IceCube Collaboration), Phys. Rev. Lett. **111** (2013) 021103.
- [23] M. G. Aartsen et al. (IceCube Collaboration), Phys. Rev. D **88** (2013) 112008.
- [24] M. G. Aartsen et al. (IceCube Collaboration), Science **342** (2013) 1242856.
- [25] S. Schönert, T. K. Gaisser and E. Resconi et al., Phys. Rev. D **79** (2009) 043009.
- [26] T. K. Gaisser, K. Jero, A. Karle et al., Phys. Rev. D **90** (2014) 023009.
- [27] M. G. Aartsen et al. (IceCube Collaboration), Phys. Rev. Lett. **114** (2015) 171102.
- [28] A. Christov, G. Golup and M. Rameez, this conference proceedings.
- [29] P. Pieroni for the Auger Collaboration, Proc. 33rd ICRC 2013, Rio de Janeiro, arXiv:1307.5059 [astro-ph].
- [30] A. Aab et al. (Pierre Auger Collaboration), Phys. Rev. D **91** (2015) 092008.
- [31] G. J. Feldman, R. D. Cousins, Phys. Rev. D **57** (1998) 3873; J. Conrad et al., Phys. Rev. D **67** (2003) 012002.
- [32] E. Waxman and J. N. Bahcall, Phys. Rev. D **59** (1998) 023002; Phys. Rev. D **64** (2001) 023002.
- [33] P. W. Gorham et al. (ANITA Collaboration), Phys. Rev. D **85** (2012) 049901(E).
- [34] I. Kravchenko et al. (RICE Collaboration), Phys. Rev. D **73** (2012) 082002.
- [35] I. Kravchenko et al. (RICE Collaboration), Phys. Rev. D **65** (2006) 062004.
- [36] K.-H. Kampert and M. Unger, Astropart. Phys. **35** (2012) 660.
- [37] M. Ahlers et al., Astropart. Phys. **34** (2010) 106.
- [38] P. Abreu et al. (Pierre Auger Collaboration), Astrophys. J. Lett. **755** (2012) L4.
- [39] M. G. Aartsen et al. (IceCube Collaboration), Astrophys. J. **796** (2014) 109.
- [40] S. Adrián-Martínez et al. (ANTARES Collaboration), Astrophys. J. Lett. **786** (2014) L5.
- [41] L. D. Landau, I. Ya. Pomeranchuk, Dokl. Akad. Nauk, SSSR **92** (1953) 535.
- [42] A. B. Migdal, Phys. Rev. **103** (1956) 1811.
- [43] L. G. Dedenko et al., Proc. 17th ICRC, Paris **7** (1981) 159.
- [44] X. Bertou, P. Billoir and S. Dagoret-Campagne, Astropart. Phys. **14** (2000) 121.
- [45] T. Erber, Rev. Mod. Phys. **38** (1966) 626.
- [46] B. McBreen and C. J. Lambert, Phys. Rev. D **24** (1981) 2536.
- [47] J. Abraham et al. (Pierre Auger Collaboration), Astropart. Phys. **27** (2007) 155.
- [48] J. Abraham et al. (Pierre Auger Collaboration), Astropart. Phys. **31** (2009) 399.
- [49] T. Abu-Zayyad et al. (Telescope Array Collaboration), Phys. Rev. D **88** (2013) 112005.
- [50] M. Settimo for the Pierre Auger Collaboration, Proc. 32nd ICRC, Beijing, **2**: 51 (2011).
- [51] K. Shinozaki et al., Astrophys. J. **571** (2002) L117.
- [52] A. Glushkov et al., Phys. Rev. D **82** (2010) 041101.
- [53] M. Ave, J. A. Hinton, R. A. Vazquez, A. A. Watson and E. Zas, Phys. Rev. Lett. **85** (2000) 2244.
- [54] P. Billoir, C. Roucelle, and J. C. Hamilton, astro-ph/0701583.
- [55] O. E. Kalashev, G. I. Rubtsov and S. V. Troitsky, Phys. Rev. D **80** (2009) 103006.
- [56] G. Gelmini, O. Kalashev, D. Semikoz, J. Exp. Theor. Phys. **106** (2008) 1061.

- [57] J. Ellis et al., Phys. Rev. D, **74** (2006) 115003.
- [58] D. Hooper, A. M. Taylor and S. Sarkar, Astropart. Phys., **34** (2011) 340.
- [59] M. Kachelriess, S. Ostapchenko and R. Tomas, Publ. Astron. Soc. Aust., **27** (2010) 482.
- [60] M. Aglietta, B. Alessandro, P. Antoni et al. (EAS-TOP Collaboration), Astropart. Phys. **6** (1996) 71.
- [61] G. Schatz et al. (KASCADE collaboration), Proc. 28th ICRC, Tsukuba **4** (2003) 2293.
- [62] J. Alvarez-Muniz, M. Risse, G.I. Rubtsov, B.T. Stokes for the Pierre Auger, Telescope Array and Yakutsk Collaborations, EPJ Web of Conferences **53** (2013) 01009.
- [63] M. C. Chantell et al. (CASA-MIA Collaboration), Phys. Rev. Lett. **79** (1997) 1805.
- [64] Yu. A. Fomin et al., JETP Lett. **100** (2014) 797.
- [65] O. E. Kalashev and S. V. Troitsky, JETP Letters **100** (2014) 865.
- [66] M. Ahlers and K. Murase, Phys. Rev. D **90** (2014) 023010.
- [67] J. C. Joshi, W. Winter and N. Gupta, Mon. Not. R. Astron. Soc. **439** (2014) 3414.
- [68] N. Gupta, Astropart. Phys. **48** (2013) 75.
- [69] L. A. Anchordoqui, H. Goldberg, M. H. Lynch et al., Phys. Rev. D **89** (2014) 083003.
- [70] K. Murase, M. Ahlers and B. C. Lacki, Phys. Rev. D **88** (2013) 121301.
- [71] D. Kang for the KASCADE-Grande Collaboration, Proc. 24th ECRS, Kiel, (2014) in press.
- [72] M. G. Aartsen et al. (IceCube Collaboration), Phys. Rev. D **87** (2013) 062002.
- [73] M. Risse and P. Homola, Mod. Phys. Lett. A, **22** (2007) 749.
- [74] A. De Angelis, G. Galanti and M. Roncadelli, Mon. Not. R. Astron. Soc. **432** (2013) 3245.
- [75] M. Settimo and M. De Domenico, Proc. 33rd ICRC, Rio de Janeiro, (2013), arXiv:1307.3739 [astro-ph.HE].
- [76] A. Aab et al. (Pierre Auger Collaboration), Astrophys. J. **789** (2014) 160.
- [77] L. Breiman, J. Friedman, R. Olshen et al., Monterey (CA), Wadsworth and Brooks (1984).
- [78] R. E. Schapire, Mach. Learn. **5** (1990) 197.
- [79] J. A. Hinton and W. Hofmann, Annu. Rev. Astro. Astrophys. **47** (2009) 523.
- [80] A. Abramowski et al. (H.E.S.S. Collaboration), A&A **528** (2011) A143.
- [81] N. I. Fisher, T. Lewis and B. J. J. Embleton, *Statistical analysis of spherical data*, Cambridge Univ. Press, 1993.
- [82] P. Allison et al. (ARA Collaboration), Astropart. Phys. **35** (2012) 457.
- [83] S. W. Barwick et al. (ARIANNA Collaboration), Astropart. Phys. **70** (2015) 12.
- [84] M. G. Aartsen et al. (IceCube-Gen2 Collaboration), arXiv:1412.5106 [astro-ph.HE].
- [85] A. Margiotta for the KM3NeT Collaboration, J. Instrum. **9** (2014) C04020.
- [86] A. V. Avrorin et al., Nucl. Instrum. Meth. A **725** (2013) 23.
- [87] K.-H. Kampert, “Auger upgrade program”, this conference proceedings.
- [88] H. Sagawa (Telescope Array Collaboration), Braz. J. Phys. **44** (2014) 589.
- [89] M. Galaverni and G. Sigl, Phys. Rev. Lett. **100** (2008) 021102.
- [90] G. Rubtsov, P. Satunin and S. Sibiryakov, Phys. Rev. D **89** (2014) 123011.
- [91] G. Raffelt and L. Stodolsky, Phys. Rev. D **37** (1988) 1237.
- [92] M. Fairbairn, T. Rashba and S. V. Troitsky, Phys. Rev. D **84** (2011) 125019.